VOLUME 28 NUMBER 11
ACCOUNTS of CHEMICAL RESEARCH®
NOVEMBER 1995

Infrared Photon Echo Experiments: Exploring Vibrational Dynamics in Liquids and Glasses

A. TOKMAKOFF† AND M. D. FAYER*

Department of Chemistry, Stanford University, Stanford, California 94305

Received May 2, 1995

I. Introduction

The dynamics of the vibrations of polyatomic molecules in polyatomic solvents are fundamentally important in many chemical processes. Vibrations can also serve as probes of intermolecular interactions and dynamics in condensed-matter systems. All thermal chemical reactions involve the flow of energy (heat) into and out of molecules through the time-dependent interactions of molecular vibrations with the solvent (heat bath). A molecule is "promoted" to a transition state in a chemical reaction by fluctuations in its molecular structure caused by dynamical interactions with the solvent. To understand many processes in liquids and solids, it is necessary to examine the time-dependent coupling of the internal mechanical degrees of freedom of a molecule (vibrations) to the solvent. In an isolated molecule, vibrations are time-independent eigenstates with time-independent eigenvalues (energy levels). In a condensed-matter system, at any temperature above $T = 0$, the system contains heat. Therefore, molecules are continually moving. Since intermolecular interactions depend on orientation and distance, the interactions are inherently time dependent. Thus the eigenvalues and eigenfunctions are time dependent; they are constantly fluctuating. These fluctuations are intimately involved in chemical processes, and they can also be used to understand dynamics of the solvent and the nature of solute/solvent interactions.

Vibrational spectra of even large molecules reveal beautiful structure, a large number of lines that can be assigned to the various types of motions that occur in a molecule. The position of the spectroscopic peak associated with a particular mode yields the energy of the vibration, but even a well-resolved vibrational line does not generally provide information on dynamics. In principle, dynamical information is contained in a spectroscopic line shape. Vibrational line shapes in condensed phases contain all of the details of the interactions of a normal mode with its environment. These interactions include the important microscopic dynamics, intermolecular couplings, and involve the time scales of the solvent evolution that modulate the energy of a transition. However, the line shape also includes the essentially static structural perturbations associated with the distribution of local solvent configurations (inhomogeneous broadening).

An infrared absorption spectrum or Raman spectrum gives frequency-domain information on the ensemble-averaged interactions that couple to the states involved in the transition.[1-3] Line shape analysis of vibrational transitions has long been recognized

Andrei Tokmakoff was born in Sacramento, CA, in 1967. He obtained a B.S. (1989) in chemistry from California State University at Sacramento in 1989 and a Ph.D. (1995) in chemistry from Stanford University. He is presently a Humboldt Fellow postdoctoral researcher at the Technical University of Munich.

Michael D. Fayer was born in Los Angeles, CA, in 1947. He obtained a B.S. (1969) and a Ph.D. (1974) in chemistry from the University of California at Berkeley. He joined the faculty at Stanford University in 1974 and has been a full professor there since 1984. His research interests include dynamics and intermolecular interactions in condensed-matter systems and supercritical fluids, investigated with ultrafast nonlinear visible and infrared optical methods and theory.

† Present address: Physik Department, Technische Universität München D85748 Garching, Germany.

(1) Gordon, R. G. *J. Chem. Phys.* **1965**, *43*, 1307.
(2) Gordon, R. G. *Adv. Magn. Reson.* **1968**, *3*, 1.
(3) Berne, B. J. In *Physical Chemistry: An Advanced Treatise*; Henderson, D., Ed.; Academic Press: New York, 1971; Vol. VIIIB.

0001-4842/95/0128-0437$09.00/0

as a powerful tool for extracting information on molecular dynamics in condensed phases.[4,5] The difficulty with determining the microscopic dynamics from a spectrum arises because linear spectroscopic techniques have no method for separating the various contributions to the vibrational line shape. The IR absorption or Raman line shape represents a convolution of the various dynamic and static contributions to the observed line shape. In some cases, polarized Raman spectra can be used to separate orientational and vibrational dynamics from the line shape, yet as with all linear spectroscopies, contributions from inhomogeneous broadening cannot be eliminated.[6]

To completely understand a vibrational line shape, a series of experiments are required to characterize each of its static and dynamic components. These experiments can be effectively accomplished in the time domain, where well-defined techniques exist for measuring the various fundamental processes. Nonlinear vibrational spectroscopy can be used to eliminate static inhomogeneous broadening from IR and Raman line shapes.[6] Techniques such as the infrared photon echo[7-9] and the Raman echo[10-13] can determine the homogeneous vibrational line shape, which contains the important microscopic dynamics, even when the line shape is masked by inhomogeneous broadening.

Below, we present the temperature-dependent vibrational dynamics of the triply degenerate T_{1u} CO stretching mode of tungsten hexacarbonyl ($W(CO)_6$) in the molecular glass-forming liquids 2-methyltetrahydrofuran (2-MTHF), 2-methylpentane (2-MP), and dibutyl phthalate (DBP). Two aspects of the vibrational line shapes are discussed in detail. Initially, we compare the behavior of the homogeneous line widths in the glasses and the transition to the room temperature liquids, using picosecond IR photon echo experiments. The temperature dependence of the vibrational dephasing and the degree of inhomogeneity as the liquids approach room temperature are discussed. The temperature dependence of the homogeneous vibrational line width in each of the three glassy solvents is T^2, but the behavior is distinct in each of the liquids. While in 2-MP the vibrational line is homogeneously broadened at room temperature, the line in DBP is massively inhomogeneously broadened even in the room temperature liquid.

Following the comparison of the temperature-dependent dephasing in the three solvents, one of the systems, $W(CO)_6$ in 2-MP, is analyzed in greater detail. The contributions to the vibrational line shape from different dynamic processes are delineated by combining the results of photon echo measurements of the homogeneous line shape[8] with pump–probe measurements of the lifetime and reorientational dynamics.[14] This combination of measurements allows the decomposition of the total homogeneous vibrational line shape into the individual components of pure dephasing (T_2^*), population relaxation (T_1), and orientational relaxation. The results demonstrate that each of these can contribute significantly, but to varying degrees at different temperatures.

II. Infrared Vibrational Photon Echo Experiments

A. The Nature of the Experiment. The picosecond infrared vibrational photon echo experiment is a time-domain nonlinear experiment that can effectively extract the homogeneous vibrational line shape even when the inhomogeneous line width is thousands of times wider than the homogeneous width. The echo technique was originally developed as the spin echo in magnetic resonance in 1950.[15] In 1964, the method was extended to the optical regime as the photon echo.[16] Since then photon echoes have been used extensively to study electronic excited state dynamics in many condensed-matter systems. For experiments on vibrations, a source of picosecond IR pulses is tuned to the vibrational transition of interest. The echo experiment involves a two-pulse excitation sequence. The first pulse puts each solute molecule's vibration into a superposition state, which is a mixture of the $v = 0$ and $v = 1$ vibrational levels. Each vibrational superposition has a microscopic electric dipole associated with it. This dipole oscillates at the vibrational transition frequency. Immediately after the first pulse, all of the microscopic dipoles in the sample oscillate in phase. Because there is an inhomogeneous distribution of vibrational transition frequencies, the individual dipoles oscillate with some distribution of frequencies. Thus, the initial phase relationship is very rapidly lost. This is referred to as the free induction decay. After a time, τ, a second pulse, traveling along a path making an angle θ with that of the first pulse, passes through the sample. This second pulse changes the phase factors of each vibrational superposition state in a manner that initiates a rephasing process. At time τ after the second pulse, the sample emits a third coherent pulse of light. The emitted pulse propagates along a path that makes an angle 2θ with the path of the first pulse (see Figure 1). The third pulse is the photon echo. It is generated when the ensemble of microscopic dipoles is rephased at time 2τ. The phased array of microscopic dipoles behaves as a macroscopic oscillating dipole, which generates an IR pulse of light. A free induction decay (inhomogeneous frequency distribution) again destroys the phase relationships, so only a short pulse of light is generated.

The rephasing at 2τ has removed the effects of the inhomogeneous broadening. However, fluctuations due to coupling of the vibrational mode to the heat bath (solvent) cause the oscillation frequencies to fluctuate. Thus, at 2τ there is not perfect rephasing.

(4) Yarwood, J. *Annu. Rep. Prog. Chem., Sect. C* **1979**, *76*, 99.
(5) Rothschild, W. G. *Dynamics of Molecular Liquids*; John Wiley and Sons: New York, 1984.
(6) Loring, R. F.; Mukamel, S. *J. Chem. Phys.* **1985**, *83*, 2116.
(7) Zimdars, D.; Tokmakoff, A.; Chen, S.; Greenfield, S. R.; Fayer, M. D.; Smith, T. I.; Schwettman, H. A. *Phys. Rev. Lett.* **1993**, *70*, 2718.
(8) Tokmakoff, A.; Zimdars, D.; Sauter, B.; Francis, R. S.; Kwok, A. S.; Fayer, M. D. *J. Chem. Phys.* **1994**, *101*, 1741.
(9) Tokmakoff, A.; Kwok, A. S.; Urdahl, R. S.; Francis, R. S.; Fayer, M. D. *Chem. Phys. Lett.* **1995**, *234*, 289.
(10) Vanden Bout, D.; Muller, L. J.; Berg, M. *Phys. Rev. Lett.* **1991**, *67*, 3700.
(11) Muller, L. J.; Vanden Bout, D.; Berg, M. *J. Chem. Phys.* **1993**, *99*, 810.
(12) Inaba, R.; Tominaga, K.; Tasumi, M.; Nelson, K. A.; Yoshihara, K. *Chem. Phys. Lett.* **1993**, *211*, 183.
(13) Vanden Bout, D.; Freitas, J. E.; Berg, M. *Chem. Phys. Lett.* **1994**, *229*, 87.
(14) Tokmakoff, A.; Urdahl, R. S.; Zimdars, D.; Kwok, A. S.; Francis, R. S.; Fayer, M. D. *J. Chem. Phys.* **1995**, *102*, 3919.
(15) Hahn, E. L. *Phys. Rev.* **1950**, *80*, 580.
(16) Kurnit, N. A.; Abella, I. D.; Hartmann, S. R. *Phys. Rev. Lett.* **1964**, *13*, 567. Abella, I. D.; Kurnit, N. A.; Hartmann, S. R. *Phys. Rev.* **1966**, *141*, 391.

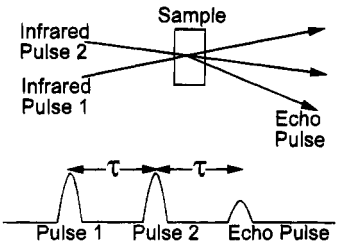

Figure 1. Schematic diagram of the infrared vibrational photon echo experiment. Two picosecond IR pulses, tuned to the vibrational transition frequency, enter the sample crossed at a small angle, θ. Because of wave vector matching, the echo pulse emerges from the sample in a unique direction, 2θ. Pulses 1 and 2 are separated by time τ. The echo is formed at time 2τ after pulse 1.

As τ is increased, the fluctuations produce increasingly large accumulated phase errors among the microscopic dipoles, and the size of the echo is reduced. A measurement of the echo intensity vs τ, the delay time between the pulses, is called an echo decay curve. Thus the echo decay is related to the fluctuations in the vibrational frequencies, not the inhomogeneous spread in frequencies. The Fourier transform of the echo decay is the homogeneous line shape.[17] For example, if the echo decay is an exponential, the line shape is a Lorentzian with a width determined by the exponential decay constant. The vibrational photon echo makes the vibrational homogeneous line shape an experimental observable. In fact, the echo decay measures directly the decay of the system's off-diagonal density matrix elements and is the most fundamental observable.

To obtain a physical feel for the manner in which the echo experiment can reveal homogeneous fluctuations in spite of a broad inhomogeneous spread of transition frequencies, consider the following foot race.[18] Initially, all the runners are lined up at the starting line. At $t = 0$ the starting gun (analogous to the first IR pulse) is fired, and the runners take off down the track. After running for some time, the faster runners have pulled out in front, and the slower runners are somewhat behind. The runners are no longer in a line because of the inhomogeneity in their speeds. At time τ, the gun is again fired (analogous to the second laser pulse), and everyone turns around and runs back toward the starting line. If each runner maintains a constant speed, out and back, then all the runners will cross the starting line exactly in line again. When the second gun was fired, the faster runners were farther away from the starting line than the slower runners, but since they run faster, the differences in distances are exactly made up for by the differences in speeds. At the starting line, the group is rephased; the inhomogeneity in speeds has been nullified. If the runners do not run at exactly constant speeds, but each runner has some fluctuation in speed about his average (homogeneous fluctuations), then the runners will not cross the starting line exactly in a line. There will not be perfect rephasing. A snapshot of the group as it crosses the starting line will reveal the small fluctuations in the runners' speeds, in spite of the large inhomogeneous distribution of speeds. In the same manner, the vibrational photon echo experiment reveals the fluctuations in the vibrational transition frequency in spite of the large inhomogeneous distribution of vibrational energies.

B. Experimental Procedures. Vibrational photon echo experiments require tunable IR pulses with durations of ~1 ps and energies of ~1 μJ. These can be produced with systems based on conventional picosecond lasers using an optical parametric amplifier (frequency difference mixing) to generate the IR pulses. However, the experiments described below were performed using a different approach. The vibrational photon echoes were performed with infrared pulses at ~5 μm (2000 cm^{-1}) generated by the Stanford superconducting-accelerator-pumped free electron laser (FEL). The FEL generates Gaussian pulses that are transform limited with pulse duration that is adjustable between 0.7 and 2 ps. The pulse length and spectrum are monitored continuously with an autocorrelator and grating monochromator.

Acquisition of data requires manipulation of the unusual FEL pulse train. The FEL emits a 2 ms macropulse at a 10 Hz repetition rate. Each macropulse consists of the picosecond micropulses at a repetition rate of 11.8 MHz (84 ns pulse separation). The micropulse energy at the input to experimental optics is ~0.5 μJ. In vibrational experiments, virtually all power absorbed by the sample is deposited as heat. To avoid sample-heating problems, micropulses are selected out of the macropulse at a reduced frequency of 50 kHz. Careful studies of power dependence and repetition rate dependence of the data were performed. It was determined that there were no heating or other unwanted effects when data was taken with pulse energies of ~15 nJ for the first pulse and ~80 nJ for the second pulse and an effective repetition rate of 1 kHz (50 kHz during each macropulse).

The same experimental apparatus was used to measure the vibrational lifetime (T_1) and the orientational relaxation dynamics. This is done with a pump–probe (transient absorption) experiment. In the experimental pulse sequence shown in Figure 1, infrared pulse 2 is the pump pulse and infrared pulse 1 is the probe pulse. The change in the transmission through the sample of the probe pulse is monitored as a function of the delay after the pump pulse. If the pulses have the same polarization, a biexponential decay is observed. The slow component is T_1, and the fast component yields the orientational relaxation rate. If the probe pulse is set to the magic angle polarization (~54°), the effect of orientational relaxation is removed from the signal, and a single exponential, decaying with the vibrational lifetime, is observed.

Vibrational photon echo and pump–probe data were taken on the triply degenerate T_{1u} asymmetric CO stretching mode of $W(CO)_6$. Solutions of $W(CO)_6$ in the glass-forming liquids were made to give a peak optical density of 0.8 with thin path lengths. Concentrations varied from 0.6 mM with a 200 μm path length for 2-MP to 4 mM with a 400 μm path length for DBP. (The difference arises because of the much broader inhomogeneous line found in DBP.) These solutions correspond to mole fractions of $\leq 10^{-4}$ and are dilute enough to eliminate Förster resonant energy transfer. The temperatures of the samples were controlled to ±0.2 K using a closed-cycled He refrig-

(17) Farrar, T. C.; Becker, D. E. *Pulse and Fourier Transform NMR*; Academic Press: New York, 1971. Skinner, J. L.; Andersen, H. C.; Fayer, M. D. *J. Chem. Phys.* **1981**, *75*, 3195.

(18) Hahn, E. L. *Phys. Today* **1953**, *6*, 4. Brewer, R. G.; Hahn, E. L. *Sci. Am.* **1984**, *251*, 50.

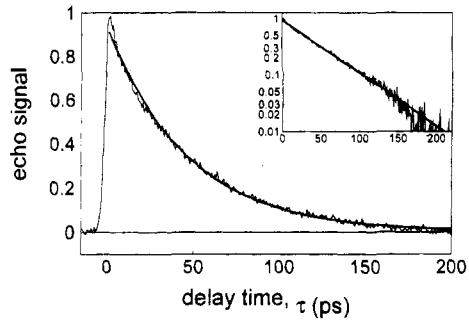

Figure 2. Photon echo decay data for the CO asymmetric stretching mode (T_{1u}) of $W(CO)_6$ in 2-methylpentane glass at 10 K. The homogeneous line width determined by the echo decay is 1.3 GHz (0.04 cm^{-1}), in contrast to the absorption line, which is inhomogeneously broadened to 310 GHz (10.3 cm^{-1}).

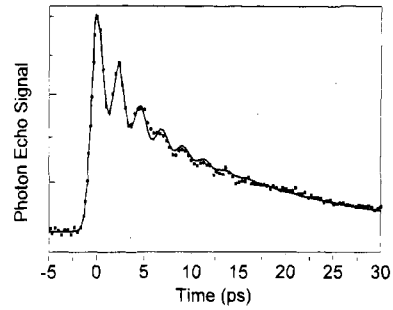

Figure 3. Vibrational photon echo decay obtained using a 0.7 ps pulse that has a bandwidth that exceeds the anharmonic shift of vibrational levels for the asymmetric CO stretching mode of $W(CO)_6$ in dibutylphthalate glass at 10 K. The fit is to a theoretically derived expression that describes the homogeneous dephasing of a three-level vibrational coherence with beating at the anharmonic frequency splitting.

erator. After equilibration, the temperature gradient across the sample never exceeded ±0.2 K.

III. Experimental Results

A. Vibrational Photon Echo Decays. The photon echo experiment is a line-narrowing experiment that measures T_2, the vibrational *homogeneous* dephasing time. The decay of the photon echo is the Fourier transform of the homogeneous spectrum. For an echo decay that is an exponential, i.e.,

$$I(t) = I_0 \exp(-4\tau/T_2) \quad (1)$$

the Fourier transform is a Lorentzian homogeneous line having width $1/(\pi T_2)$. The echo signal decays four times as fast as the dephasing time, due to the echo rephasing at 2τ, and the intensity decaying twice as fast as the polarization. Figure 2 displays photon echo data for $W(CO)_6$ in 2-MP taken in the low-temperature glass at 10 K. The inset shows a log plot of the data. The decay is exponential, indicating that the homogeneous line is a Lorentzian. At this temperature, the absorption line width is 10.3 cm^{-1} (310 GHz). In contrast T_2 = 240 ps, yielding a homogeneous line width of 1.3 GHz. Thus the absorption line is massively inhomogeneously broadened.

Figure 3 displays data taken using 0.7 ps pulses in the solvent DBP.[9] When the pulse duration is made shorter, the associated bandwidth of the transform-limited pulse is larger. When the bandwidth of the excitation pulses exceeds the vibrational anharmonicity, then population can be excited to higher vibrational levels. The extent of vibrational up-pumping is limited only by the magnitude of the vibrational anharmonic frequency splitting, Δ, relative to the laser bandwidth, Ω. For the case where $\Delta \approx \Omega$, short pulse excitation will create a three-level coherence involving the v = 0, 1, and 2 vibrational levels. The expected photon echo signal can be described for an unequally spaced three-level system using a semiclassical perturbative treatment of the third-order nonlinear polarizability in the Bloch limit.[19] The three-level system is spaced by the frequencies ω_{10} and ω_{21}, where $\omega_{10} = \omega_{21} + \Delta$ and $\Delta \ll \omega_{10}$ and ω_{21}. The transition frequencies ω_{10} and ω_{21} lie within the bandwidth of the pulses. The theoretical derivation shows that the echo signal envelope decays in proportion to the dephasing rates of the $v = 0 \rightarrow 1$ and $v = 1 \rightarrow 2$ transitions, with exponentially damped beats observed at the frequency splitting, Δ. For the narrow bandwidth case, eq 1 is recovered.

As can be seen from Figure 3, the decay is consistent with the expected decay of a three-level vibrational coherence. The solid line was obtained from the theoretical calculation. The decay is modulated at a 2.3 ps frequency, which is constant within error over all temperatures. On the basis of the average of several data sets, the vibrational anharmonic splitting is $\Delta = 14.7\ cm^{-1} \pm 0.3\ cm^{-1}$. This splitting is in accord with the value of 15 $cm^{-1} \pm 1\ cm^{-1}$ recently obtained by Heilweil and co-workers from observation of the $v = 1 \rightarrow 2$ and $v = 2 \rightarrow 3$ transitions of the asymmetric CO stretching mode of $W(CO)_6$ in hexane using transient infrared absorption.[20] The agreement between the anharmonicity obtained from the beat frequency and that obtained by transient absorption confirms the interpretation of the beats as arising from the multilevel coherence of the anharmonic oscillator. The echo decay data also provide the homogeneous dephasing times for the two transitions involved in the multilevel coherence. These experiments are the first to determine the homogeneous vibrational line width for both the $v = 0 \rightarrow 1$ and $v = 1 \rightarrow 2$ transitions and provide a direct method for obtaining the anharmonicity of the vibrational potential.

B. Temperature Dependence of Vibrational Dephasing. 1. Below the Glass Transition Temperature. The results of temperature-dependent photon echo experiments on the T_{1u} mode of $W(CO)_6$ in the three glass-forming liquids are shown in Figure 4. The homogeneous line width, $\Gamma = 1/(\pi T_2)$, is shown, derived from fits with the photon echo signal decaying exponentially as eq 1. Data on 2-MTHF were taken from 10 K up to 120 K, at which point the decay rate exceeded the instrument response. With the same time resolution, echo data in the other liquids were observable up to room temperature. The data on DBP (discussed above) were taken with 0.7 ps pulses. At temperatures above 150 K, where the decays are fast, the presence of the beats on the decays introduced substantial uncertainty into the determination of the vibrational line width for the $v = 0 \rightarrow 1$ level.

The temperature dependence of the homogeneous line width increases monotonically in the glass. Above the glass transition temperature, the line widths in

(19) Mukamel, S.; Loring, R. F. *J. Opt. Soc. B* **1986**, *3*, 595. Yan, Y. J.; Mukamel, S. *J. Chem. Phys.* **1991**, *94*, 179.
(20) Arrivo, S. M.; Dougherty, T. P.; Grubbs, W. T.; Heilweil, E. J. *Chem. Phys. Lett.* **1995**, *235*, 247.

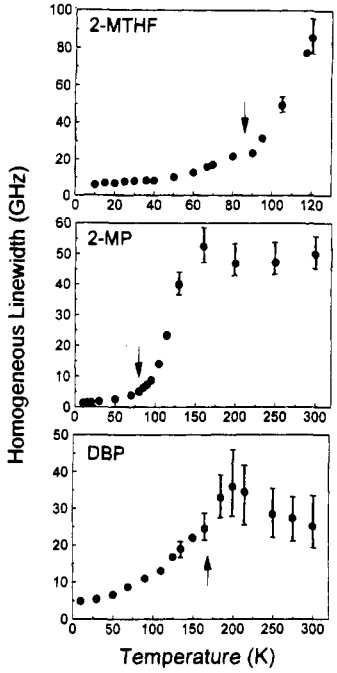

Figure 4. Temperature dependence of the homogeneous line widths of the T_{1u} CO stretching mode of $W(CO)_6$ in 2-MTHF, 2-MP, and DBP, determined from infrared photon echo experiments using eq 1. Arrows mark the glass transition temperatures. Note the different temperature and line width scales.

2-MTHF (T_g = 86 K) and 2-MP (T_g = 80 K) rise rapidly in a manner that appears thermally activated. In 2-MP, the rapid increase in dephasing rate slows above 130 K and becomes temperature independent. In DBP (T_g = 169 K), the line width appears to decrease with temperature above 200 K although the error bars are large enough that it is possible that the temperature dependence is essentially flat.

The temperature dependences of the homogeneous vibrational line widths in the three glasses are compared using a reduced variable plot in Figure 5a. Although the absolute line widths for each system may vary, this is a reflection of the strength of coupling of the transition dipole to the bath and can be removed by normalization to the line width at the glass transition temperature. Likewise, using a reduced temperature, T/T_g, allows thermodynamic variables that contribute to determining the glass transition to be normalized. Such normalization allows comparison of the functional form of the temperature dependences, independent of differences in T_g and coupling strengths. Figure 5a shows that the temperature dependences of the homogeneous line widths are identical in the three glasses and are well described by a power law of the form

$$\Gamma(T) = \Gamma_0 + AT^{\alpha} \qquad (2)$$

The offset at 0 K, Γ_0, represents the line width due to the low-temperature vibrational lifetime. A fit to eq 2 for all temperatures below the glass transition is shown in Figure 5a and yields an exponent of $\alpha = 2.1 \pm 0.2$ and $\Gamma_0/\Gamma(T_g) = 0.24 \pm 0.02$. At temperatures above $\sim 1.2T_g$, the line widths of the three liquids diverge from one another. All of the liquids were individually fitted to eq 2. The results demonstrate that the temperature dependence is well described by a power law of the form T^2.

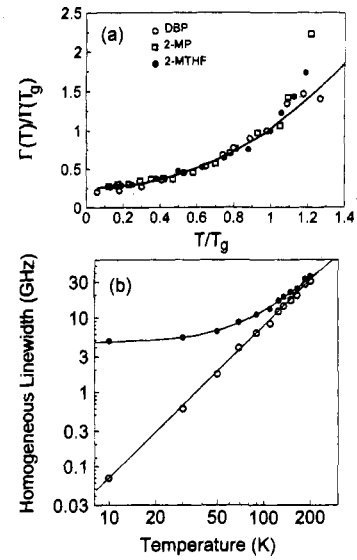

Figure 5. (a) Comparison of the homogeneous infrared line width in three organic glasses. The homogeneous line width normalized to the line width at the glass transition temperature to remove the coupling strength is plotted against the reduced temperature. The temperature dependence follows a T^2 power law plus a low-temperature lifetime contribution. (b) Homogeneous line width of the T_{1u} mode of $W(CO)_6$ in DBP between 10 and 200 K. The homogeneous line widths are shown in solid circles, and the corresponding data with the low-temperature lifetime of $T_1(0\ K) = 33$ ps removed are shown with open circles. The data fit a T^2 power law.

Because of its high glass transition temperature, DBP allows the largest temperature range over which to observe the power law. The data are presented in two ways in Figure 5b. The solid circles are the data, and the line through them is a fit to eq 2. To show more clearly the power law temperature dependence, the open circles are the data with the low-temperature line width Γ_0 (corresponding to a vibrational lifetime $T_1(0\ K) = 33$ ps) subtracted out. The line through the data is T^2. It can be seen that the power law describes the data essentially perfectly over a change of line width of ~500 from 10 to 200 K.

The dynamics of optical dephasing in glasses[21] are generally interpreted within the model of two-level systems, initially proposed to describe their anomalous low-temperature heat capacities.[22,23] In this model, pure dephasing dynamics are described in terms of phonon-induced transitions between structural potential wells. At temperatures above the Debye frequency of the glass, a power law of T^2 is theoretically predicted for dephasing due to two-phonon (Raman) scattering processes between potential wells.[21] Huber has pointed out that, in glasses, this temperature dependence is expected above an effective Debye temperature, which can often be 2–10 times lower than the true Debye temperature.[24] The $\alpha \approx 2$ temperature dependence is almost universally seen for the high-temperature dephasing of electronic transitions in a variety of glasses.[21]

Figure 5 demonstrates that the underlying temperature dependence of the vibrational homogeneous dephasing measured with the photon echoes is, in fact,

(21) Macfarlane, R. M.; Shelby, R. M. *J. Lumin.* **1987**, *36*, 179.
(22) Anderson, P. W.; Halperin, B. I.; Varma, C. M. *Philos. Mag.* **1972**, *25*, 1.
(23) Phillips, W. A. *J. Low Temp. Phys.* **1972**, *7*, 351.
(24) Huber, D. L. *J. Non-Cryst. Solids* **1982**, *51*, 241.

identical in the three glasses studied here and is described by a power law T^2. The results presented here are the first to examine the temperature dependence of vibrational dephasing in organic glasses. The observation of the T^2 dependence suggests that these glasses are in the high-temperature limit above 10 K and that the temperature dependence of vibrational pure dephasing may be universal in all high-temperature glasses. This would be consistent with dephasing caused by Raman (two-quantum) phonon scattering.

2. Above the Glass Transition Temperature. The temperature dependences of the rate of dephasing in 2-MP and 2-MTHF (Figure 4) both show a gradual increase with temperature until shortly after the glass transition, at which point a rapid increase in dephasing is observed. Coincidentally, the glass transition temperatures for 2-MP (T_g = 80 K) and 2-MTHF (T_g = 86 K) are very similar. Thus, the rapid increase in dephasing can be explained by two possible phenomena: either by the emergence of new modified relaxation dynamics above the glass transition or by thermally activated dephasing through coupling to a low-frequency intramolecular mode of $W(CO)_6$. If one of the low-frequency modes of $W(CO)_6$ is quadratically coupled to the T_{1u} mode, thermal population of this low-frequency mode would result in thermally activated dephasing of the T_{1u} mode. For this mechanism, the break in the functional form of the temperature dependence would be independent of T_g. The temperature dependence of the T_{1u} vibrational line width in DBP shows no dramatic change near 90 K, demonstrating that such a mechanism is not the cause of the rapid increase in dephasing rates near 90 K in the other glasses. Rather, since the mechanism is dependent on the solvent, the dephasing is dictated by the particular temperature-dependent dynamics of the solvent. At temperatures above the glass transition, the normalized line widths in the three liquids diverge from each other, indicating the emergence of distinct relaxation processes in the various liquids.

In 2-MTHF and in 2-MP below 150 K, the echo decays yield a homogeneous line width that is much narrower than the width of the absorption spectrum. These results demonstrate that the vibrational lines of these system are inhomogeneously broadened in the glasses and supercooled liquids. As shown below, in 2-MP the $W(CO)_6$ T_{1u} line becomes homogeneously broadened at room temperature. However, in DBP the line is clearly inhomogeneous at all temperatures. The homogeneous line width at 300 K is $\sim$1 cm^{-1}, while the absorption spectrum line width is 26 cm^{-1}. This is the first conclusive evidence for intrinsic inhomogeneous broadening of a vibrational line in a room temperature liquid. Thus, even in room temperature liquids, it is not safe to assume that dynamics can be obtained by taking a vibrational spectrum and analyzing it assuming it is homogeneously broadened.

C. Contributions to the Homogeneous Line Shape in 2-MP. 1. Transition to a Homogeneously Broadened Line. The measured homogeneous vibrational line width obtained from infrared photon echo measurements (Figure 4) assumed that the echo decays as eq 1. This equation is valid in the inhomogeneous limit, when the width of the inhomogeneous distribution of homogeneous lines far exceeds the homogeneous line width Γ. This inhomogeneous limit implies that a separation of time scales exists between the fast fluctuations of homogeneous dephasing and long-time scale inhomogeneous structural evolution. Such is the case below 150 K, where the echo decays yield a homogeneous line width that is much narrower than the width of the absorption spectrum. At these temperatures, the data demonstrate with certainty that the T_{1u} vibrational line in 2-MP is substantially inhomogeneously broadened.

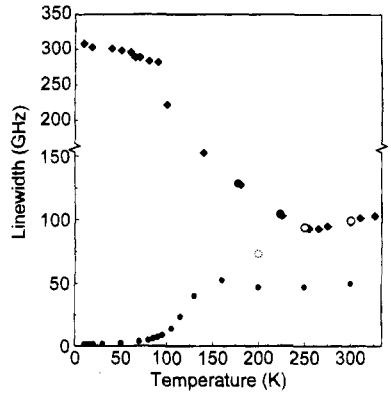

Figure 6. Temperature dependence of the homogeneous and absorption line widths for the T_{1u} mode of $W(CO)_6$ in 2-MP. The homogeneous line widths (solid circles) are taken from Figure 4. The "echo" data at 250 and 300 K are actually free induction decays that match the observed absorption line (open circles), showing that the spectra are homogeneously broadened. At 200 K (dotted circle), the homogeneous and inhomogeneous contributions to the absorption line are of equal magnitude. Below 200 K, the homogeneous line width is much narrower than the inhomogeneous width.

Above 150 K, the homogeneous line width begins to approach the measured absorption line width, as illustrated in Figure 6. Under these conditions, the time scale for the rephasing of the echo pulse is shortened by the polarization decay due to homogeneous dephasing. This causes the echo to rephase at times between τ and 2τ. Thus, the echo signal decays at a slower rate than the $4/T_2$ given by eq 1.[25,26] As the homogeneous dephasing time T_2 decreases, the rephasing of the echo is shifted to shorter times. In the limit that the absorption line is homogeneously broadened, a free induction decay (FID) will be observed along the echo direction. If the homogeneous line is a Lorentzian, then an exponential decay with a decay constant of $2/T_2$ will be observed.[26]

The data above 150 K reflect this transition to a homogeneously broadened line. If near room temperature the measured echo data are actually FIDs from a homogeneously broadened line, the decay constants $2/T_2$ yield a line width given by the open circles in Figure 6. The FID line widths match the measured absorption line widths exactly, demonstrating that the line is homogeneously broadened for temperatures $\geq$250 K. Notice that the absorption line width, which narrows for temperatures up to 200 K, actually broadens slightly for higher temperatures, in a manner that precisely follows the echo data. Without experimentally time resolving the rephasing of the echo pulse, it is not possible to determine from an echo experiment alone if the observable is a true echo decay, a FID, or an intermediate case. However, a comparison to the absorption spectrum provides a test. Since treating the point at 160 K as a FID still results

(25) Cho, M.; Fleming, G. R. *J. Chem. Phys.* **1993**, *98*, 2848.
(26) Joo, T.; Albrecht, A. C. *Chem. Phys.* **1993**, *176*, 233.

in a line width that is narrower than the absorption line, this point corresponds to a true photon echo. The point at 200 K represents the transition between a homogeneous and an inhomogeneous absorption line shape.

In liquids, the distinction between homogeneous and inhomogeneous broadening is a matter of definitions and time scales. A photon echo experiment measures the homogeneous line shape, which arises from fast fluctuations of the medium that cause rapid fluctuations of the vibrational energy levels. In a liquid, the homogeneous line width can be much narrower than the inhomogeneous line width even at room temperature, as shown above for $W(CO)_6$ in DBP. However, on some time scale, a molecule in a liquid will sample all possible solvent environments that give rise to the inhomogeneous spectrum. Therefore, on a time scale long compared to the homogeneous dephasing time, the vibrational spectrum of a molecule will spectrally diffuse throughout the full inhomogeneous line, provided the excited state lifetime is sufficiently long. The slower dynamic processes that give rise to spectral diffusion are essentially static on the time scale of the homogeneous dephasing and appear as part of the quasi-static inhomogeneous background. This quasi-static distribution of vibrational energies is rephased in a photon echo experiment and does not contribute to the homogeneous line width.

2. Components of the Homogeneous Line. Pump–probe studies of the population dynamics of the T_{1u} mode of $W(CO)_6$ in 2-MP have observed dynamics that contribute to the infrared absorption line shape.[14] In addition to pure dephasing (energy fluctuations), population relaxation and orientational relaxation of the initially excited dipole contribute to the homogeneous line width. By combining the photon echo and pump–probe data, all of the dynamics that contribute to the homogeneous line shape can be obtained.[27] Equation 1 gives a Lorentzian line shape, and contributions to the full line width at half maximum (FWHM) are additive:

$$\Gamma = 1/(\pi T_2) = 1/(\pi T_2^*) + 1/(2\pi T_1) + \Gamma_{or} \quad (3)$$

The orientational contribution to the infrared line shape due to isotropic orientational diffusion of the dipole is given by

$$\Gamma_{or} = 2D_{or}/\pi \quad (4)$$

where D_{or} is the orientational diffusion constant. Using pump–probe measurements of the orientational diffusion constant D_{or} and the population relaxation time T_1,[14] the contribution due to pure dephasing can be determined from the homogeneous line width. (There are a number of subtle issues involved in considering the influence of orientational relaxation on the photon echo decay. A full discussion of these in relation to the material presented below is given in ref 27.)

Figure 7 displays the decomposition of the temperature dependence of the homogeneous vibrational line width into its three dynamic components. At low temperatures, the lifetime is the dominant contribution. At high temperatures, pure dephasing is the dominant contribution. Only at intermediate temperatures does orientational relaxation make a substantial contribution. The line width contribution from lifetime broadening remains significant until ~50 K. Above 50 K, pure dephasing and orientational relaxation make the major contributions to the line width. Orientational relaxation does not dominate in any temperature range, but makes its largest percentage contribution around 100 K. By 100 K, the pure dephasing is a substantially larger contribution than either the lifetime or the orientational relaxation. Above ~150 K, pure dephasing overwhelms the other contributions to the homogeneous line width.

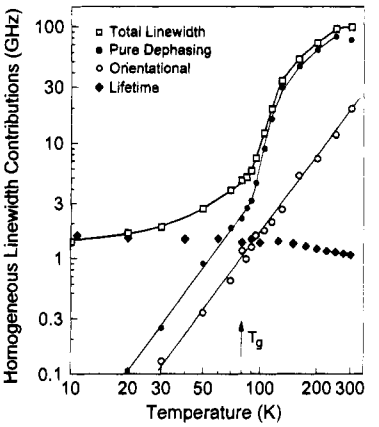

Figure 7. Log–log plot of the dynamic contributions to the homogeneous vibrational line width of the T_{1u} mode of $W(CO)_6$ in 2-MP: (□) total line width; (◆) lifetime contribution; (●) pure dephasing contribution; (○) orientational contribution. The vibration lifetime dominates the homogeneous line width at the lowest temperatures and is only mildly temperature dependent. At high temperatures, pure dephasing dominates the homogeneous line width. Orientational relaxation never dominates but makes significant contributions to the line width at intermediate temperatures. The orientational contribution, shown with a T^2 power law line, is continuous over all temperatures. The temperature dependence of the pure dephasing is the same as the orientational relaxation in the glass. The line through the pure dephasing data is a fit to eq 6. Error bars on the total line width, lifetime, and pure dephasing are approximately the size of the symbols. The orientational error bars vary from the size of the symbols at high temperature to ±50% at 30 K.

At low temperature, where the contributions from pure dephasing and orientational relaxation are negligible, the contribution to the line width from the lifetime (from pump–probe data) and the line width determined from the decay of the echo are equal within error. This is the expected low-temperature limit for the homogeneous vibrational line width where processes caused by thermal fluctuations disappear, and only lifetime broadening is possible.

The lifetime contribution to the line width, $1/(2\pi T_1)$, appears virtually constant on the log–log plot of Figure 7. The lifetime contribution decreases by nearly 50% in going from 10 to 300 K; however, this temperature dependence is insignificant in comparison to the temperature dependences of the other phenomena. An equivalent temperature dependence of T_1 exists for $W(CO)_6$ in DBP. The mild temperature dependence of T_1 shows that it is adequate to subtract a constant, Γ_0, for the lifetime contribution when making the log–log plot in Figure 5 to display the power law temperature dependence.

From low temperature to slightly above T_g, both pure dephasing and orientational relaxation have

(27) Tokmakoff, A.; Fayer, M. D. *J. Chem. Phys.* **1995**, *103*, 2810.

power law temperature dependences. The earlier discussion of the combined dynamics in 2-MP and the other two solvents showed a T^2 temperature dependence when the lifetime contribution was taken out. Here, the contributions from both pure dephasing and orientational relaxation are shown to follow the same T^2 power law behavior in the glass. Thus the total temperature dependence, excluding T_1, is T^2 as shown in Figure 5. In addition, the power law observed for the orientational relaxation in the glass is observed to continue into the liquid. In Figure 7, a power law fit of $\alpha = 2.2 \pm 0.2$ is shown. The orientational dynamics are independent of the glass transition and distinctly nonhydrodynamic.[27] This is consistent with the results of pump–probe experiments.[14]

In Figure 7 it is seen that there is a rapid increase in pure dephasing beginning slightly above the glass transition temperature. This implies that an additional mechanism or a change in the nature of the mechanism for pure dephasing turns on, and it is linked to the glass-to-liquid transition. The onset of dynamic processes near the glass transition is often described with a Vogel–Tammann–Fulcher equation:[28–30]

$$\tau = \tau_0 \exp(B/(T-T_0)) \qquad (5)$$

This equation describes a process characterized by a time, τ, with a temperature-dependent activation energy that diverges at a temperature, T_0, which is usually below the nominal glass transition temperature ($\eta(T_g) = 10^{13}$ P). T_0 can be linked thermodynamically to an "ideal" glass transition temperature that would be measured with an ergodic observable.[28] This equation describes the temperature dependence of the viscosity of 2-MP well and gives $T_0 = 59$ K.[27]

If the Vogel–Tammann–Fulcher (VTF) equation applies to pure dephasing near and above the glass transition, then the full temperature dependence would be the sum of the low-temperature power law plus a VTF term. To test this idea, the temperature dependence of pure dephasing was fitted to

$$\Gamma^*(T) = A_1 T^{\alpha} + A_2 \exp(-B/(T-T_0^*)) \qquad (6)$$

for all temperatures below 300 K and is shown as the line through the pure dephasing data in Figure 7. The fit describes the entire temperature dependence exceedingly well and yields a reference temperature of $T_0^* = 80$ K. This reference temperature matches the laboratory glass transition temperature T_g exactly, not the ideal glass transition temperature T_0. We can thus infer that the onset of the dynamics that cause the rapid increase in homogeneous dephasing in 2-MP is closely linked with the onset of structural processes near the laboratory glass transition temperature. This may be a manifestation of the short time scale of the measurement and a reflection of the nonergodicity of the system.

The temperature dependence given by eq 6 does not describe the decrease in the pure dephasing line width observed for the 300 K point. It is possible that this can be explained by motional narrowing of the line,[31] which is consistent with the observed transition to a homogeneously broadened absorption line at 250 K.

3. Relationship to Theories of Pure Dephasing in Liquids. The data presented here can be compared with the predications of a number of theories for the temperature dependence of vibrational dephasing in liquids.[4,32–34] A large number of the theories for vibrational pure dephasing in liquids based on vibrational–transitional coupling and collision-induced frequency perturbations have obtained results that are related to viscosity. Lynden-Bell relates vibrational dephasing to translational diffusion within the liquid potential and obtains a temperature dependence $1/T_2^* \propto \varrho\eta/T$.[35] The isolated binary collision (IBC) model of Fischer and Laubereau[36] relates the line width to dephasing collision probability yielding $1/T_2^* \propto \eta T/\varrho$. The hydrodynamic model of Oxtoby[37] obtains results similar to the IBC model, $1/T_2^* \propto \eta T$.

None of these theories can describe the data in this study. Although the viscosity in liquid 2-MP increases by approximately 14 orders of magnitude between 300 and 80 K, the rate of pure dephasing changes by less than 2 orders of magnitude. These hydrodynamic theories do predict a decrease in line width with decreasing temperature, as observed for the pure dephasing of $W(CO)_6$ in 2-MP and the total homogeneous line width in DBP. The problem may be that the viscosity does not form an adequate approximation for the collision frequency,[4] or that an explicit mechanism for dephasing in a particular system may be necessary to explain the temperature dependence.

Schweizer and Chandler have calculated the vibrational dephasing due to fast interactions with the repulsive wall of the potential based on an Enskog collision time.[38] This theory predicts a temperature dependence of $1/T_2^* \propto \varrho T^{6/2} g(\sigma)$, where $g(\sigma)$, the contact value of the radial distribution function for a spherical solvent with diameter σ, may be mildly temperature dependent. This temperature dependence comes much closer to describing the pure dephasing of $W(CO)_6$ in 2-MP between 130 and 275 K, but does not reflect the rapid increase in the viscous, supercooled liquid between 80 and 130 K.

A description of vibrational dephasing above the glass transition that is valid for viscous fluids is clearly necessary. Such a theory might benefit from some of the approaches to amorphous media that are used for the theories of high-temperature dephasing in glasses. The data presented here have demonstrated the existence of continuous T^2 behavior through the glass transition with the rapid onset of an additional or modified dephasing process above the glass transition.

IV. Concluding Remarks

The development of picosecond vibrational photon echo experiments to examine condensed matter systems represents a significant extension of the field of vibrational spectroscopy. Recently we have also ap-

(28) Angell, C. A. *J. Phys. Chem. Solids* **1988**, *49*, 863.
(29) Angell, C. A. *J. Phys. Chem.* **1982**, *86*, 3845.
(30) Fredrickson, G. H. *Annu. Rev. Phys. Chem.* **1988**, *39*, 149.
(31) Kubo, R. In *Fluctuation, Relaxation, and Resonance in Magnetic Systems*; Ter Haar, D., Ed.; Oliver and Boyd: London, 1962.
(32) Oxtoby, D. W. *Adv. Chem. Phys.* **1979**, *40*, 1.
(33) Chesnoy, J.; Gale, G. M. *Adv. Chem. Phys.* **1988**, *70*, 297.
(34) Oxtoby, D. W. *Annu. Rev. Phys. Chem.* **1981**, *32*, 77.
(35) Lynden-Bell, R. M. *Mol. Phys.* **1977**, *33*, 907.
(36) Fischer, S. F.; Laubereau, A. *Chem. Phys. Lett.* **1975**, *35*, 6.
(37) Oxtoby, D. W. *J. Chem. Phys.* **1979**, *70*, 2605.
(38) Schweizer, K. S.; Chandler, D. *J. Chem. Phys.* **1982**, *76*, 2296.

plied other nonlinear experimental methods in the IR to study vibrations. We have used stimulated photon echoes and transient grating experiments. All of these methods are types of four-wave-mixing experiments. The application of four-wave-mixing experiments to the study of electronic states and nonresonant phenomena in the visible part of the spectrum has had explosive growth in the 1980s and 1990s. Vibrational spectroscopy has always gained importance because of its selectivity, i.e., its ability to look at specific, well-defined mechanical degrees of freedom of molecules. The advent of IR vibrational four-wave-mixing experiments, such as the photon echo experiments described here, will provide important tools to greatly increase our understanding of the dynamics and intermolecular interactions in molecular systems of interest in chemistry, biology, and materials science.

In principle, analysis of a vibrational line shape can provide a great deal of information on dynamics and intermolecular interactions in condensed matter systems. However, to completely characterize an infrared line shape, a combination of experimental methods is necessary to elucidate each of the dynamic and static contributions to the line. Picosecond infrared photon echo experiments were used to measure the homogeneous line shape and remove inhomogeneity. Infrared pump–probe experiments were used to measure the vibrational lifetime and orientational relaxation. The total vibrational line shape was determined by absorption spectroscopy. Together, these experiments yield a complete characterization of the dynamics that make up the homogeneous line, and the extent of inhomogeneity of the infrared absorption line.

The authors gratefully acknowledge David Zimdars, Dr. Randy Urdahl, Dr. Bernd Sauter, Rick Francis, and Dr. Alfred Kwok, who were involved in many of the experiments that are discussed and referenced in this paper. The authors thank Professor Alan Schwettman and Professor Todd Smith of the Department of Physics, Stanford University, and their groups for the opportunity to use the Stanford Free Electron Laser. We also thank Dr. Camilla Ferrante for many helpful discussions. This work was supported by the National Science Foundation (DMR93-22504), the Office of Naval Research (N00014-92-J-1227), the Medical Free Electron Laser Program (N00014-91-C-0170), and the Air Force Office of Scientific Research (F49620-94-1-0141).

AR950028T